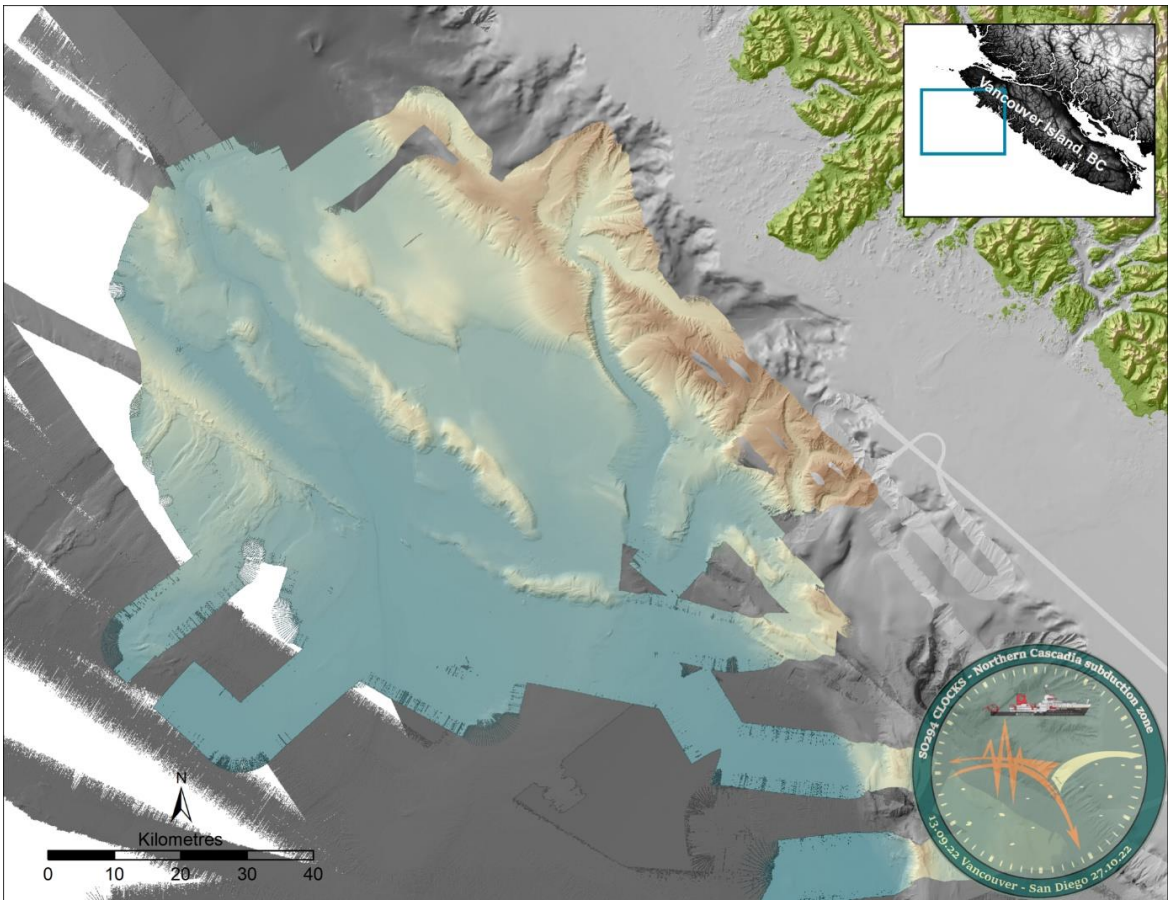

Figure 2: Multibeam bathymetry coverage of the Explorer Plate region from SO294 in color. Basemap contains data from Kung (2021) and GMRT (Ryan et al., 2009) in grey-scale.

Citation:
Kung, R. 2021. "Canada's west coast: a digital elevation model with seamless transitions between marine and coastal terrestrial environments". Natural Resources Canada. https://open.canada.ca/data/en/dataset/e6e11b99-f0cc-44f7-f5eb-3b995fb1637e [Accessed online 2022-10-09].
Ryan, W.B.F., S.M. Carbotte, J.O. Coplan, S. O'Hara, A. Melkonian, R. Arko, R.A. Weissel, V. Ferrini, A. Goodwillie, F. Nitsche, J. Bonczkowski, and R. Zemsky (2009), Global Multi-Resolution Topography synthesis, Geochem. Geophys. Geosyst., 10, Q03014, doi: 10.1029/2008GC002332

During our mapping and acoustic measurements, we also record the water column data from the multibeam sounders. This is used to detect natural fluid and gas seeps on the seabed, so-called gas plumes. These gas plumes are caused by acoustic backscatter from rising gas bubbles. To date, we have identified around 20 gas plumes in the north-eastern section of the Winona Basin in water depths ranging from 1660 m to 480 m (Figure 3).

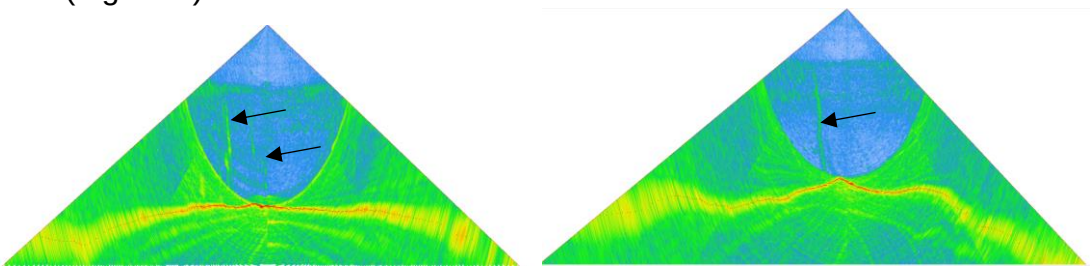

Figure 3: Examples of two acoustic water column fan-view profiles from the EM 122 multibeam sonar showing gas fares (black arrows) In the north-eastern region mapped within the Winona Basin (Image: Jessie Kehew).

Despite adverse wind and wave conditions (wind force of approximately 6-7 throughout this week), we recovered our 20 ocean bottom seismometers (OBS) and successfully backed up the data within just under 2 days.

The rest of the week was spent alternating instrument deployments with the heat probe (Figure 4) and the gravity corer. This was the first use of the heat-probe during SO294. The principle of heat-probe measurements is simple: the probe weighing ~1.5 tons consists of a topweight containing all electronics, and a 6 m long steel rod to which a temperature string of 22 individual thermal sensors is attached (Figure 4). The probe is lowered from the ship by a winch-wire to the seafloor and penetrates by its own weight into the sediment.

Figure 4: Deployment of the heat-probe (Photo: Sarah-Marie Kröger).

After penetration, frictional heating causes temperature to rise along the temperature string (Figure 5). The temperature adjustment after the probe has fully penetrated into the sediments allows estimation of the in-situ temperature and thus the temperature gradient in the subsurface. After a 7-8 minute long waiting period for the sensors to adjust to the prevailing ambient temperature in the subsurface, a controlled short thermal pulse is released and the temperature drop after this pulse is measured to calculate the thermal conductivity of the sediments (Figure 6). Together with the temperature gradient, this is then used to determine heat flow.

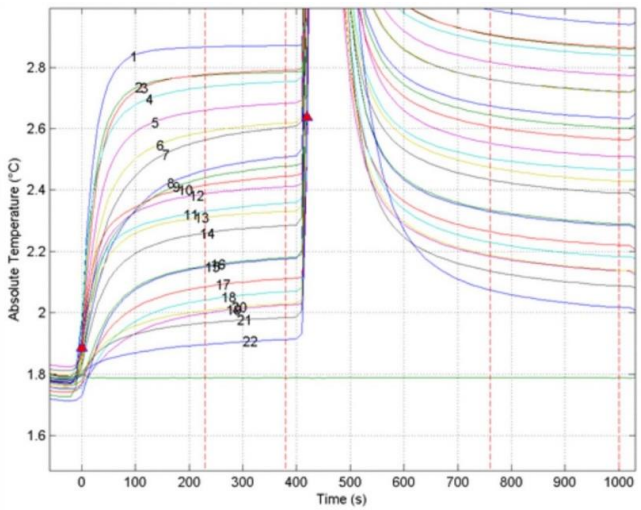

Figure 5: Example of a raw temperature record prior to calibration of a heat-probe measurement at Station P1_T01, location see figure 7. Frictional heating is followed by adaptation of the sediments to in situ temperature in the subsurface, and the decline of temperature after a controlled heat pulse indicates thermal conductivity of the sediments.

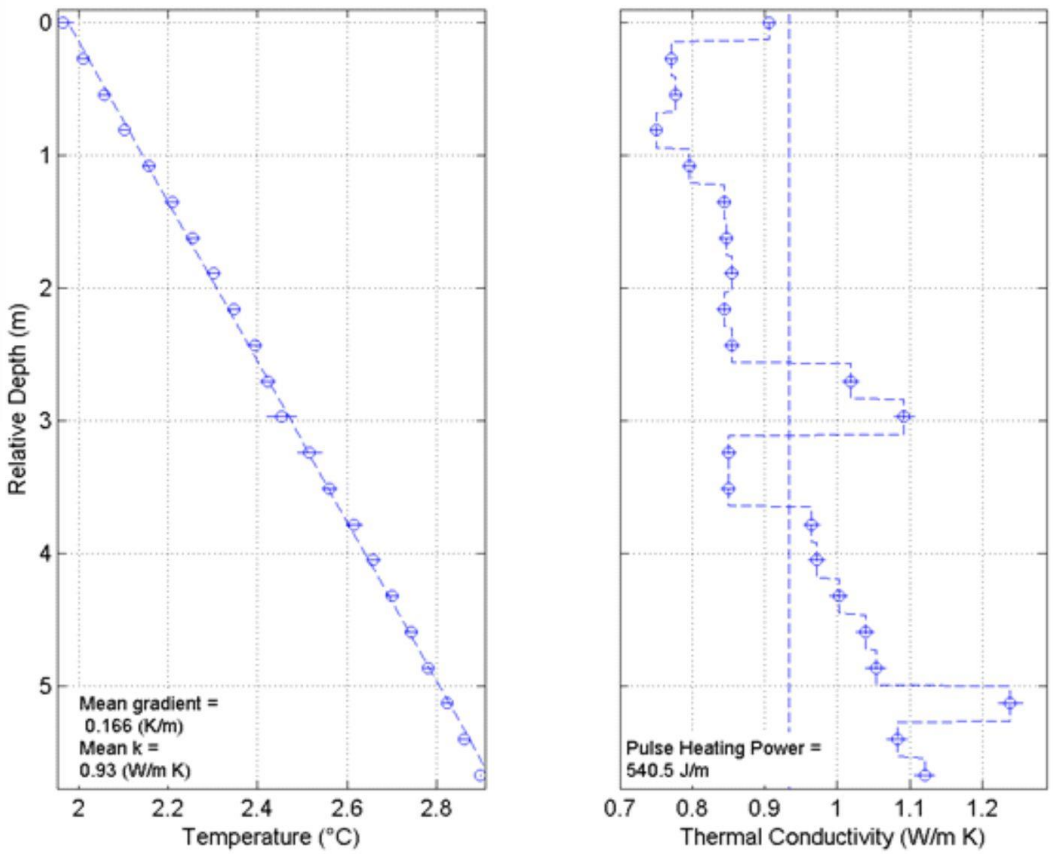

Figure 6: Left: Temperature-depth profile at station P1_T01 with calculated thermal gradient (~166°C/km). Right: Depth profile of the thermal conductivity of the sediment. Together, this results in a heat flux of 155 mW/m².

In total, we made 30 heat flux measurements along the two main seismic refraction profiles (Figure 7). The measurements were almost all successful, but it was difficult to penetrate the sediment on two ridge structures. The probe could not penetrate deep enough into the sediment there, so no heat flux data are available at these stations. However, this does not pose a problem to the overall interpretation of the temperature data, as we were able to identify the bottom simulating reflector ("BSR") across these ridge structures in our seismic data. The BSR marks the lower boundary of the gas hydrate layer and is thus equivalent to an isotherm, and thus indirectly provides clues to the heat flux.

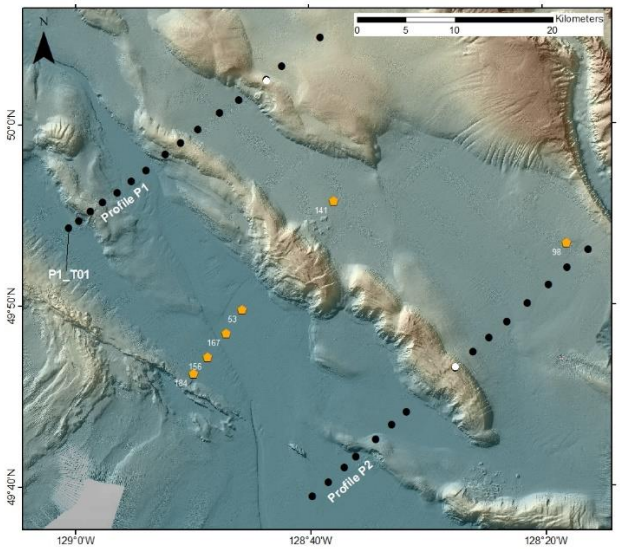

Figure 7: Map showing the heat-probe stations occupied in the Winona Basin (black points). White points mark sites of no penetration of the probe due to hard ground. For comparison, data form the international heat-flow data base (http://ihfc-iugg.org/products/global-heat-flow-database) are given including previously determined thermal gradients (orange symbols).

With a total of 12 sediment cores taken at 5 submarine slope failures (Figure 8), we have also completed the coring program in the Winona Basin on Sunday, October 9. The sediment cores were sampled for pore water with rhizones and the samples were secured on board for later measurements in the laboratory at GEOMAR. The pore fluid sub-samples are now stored in refrigerators and freezers on board until further transport to Kiel.

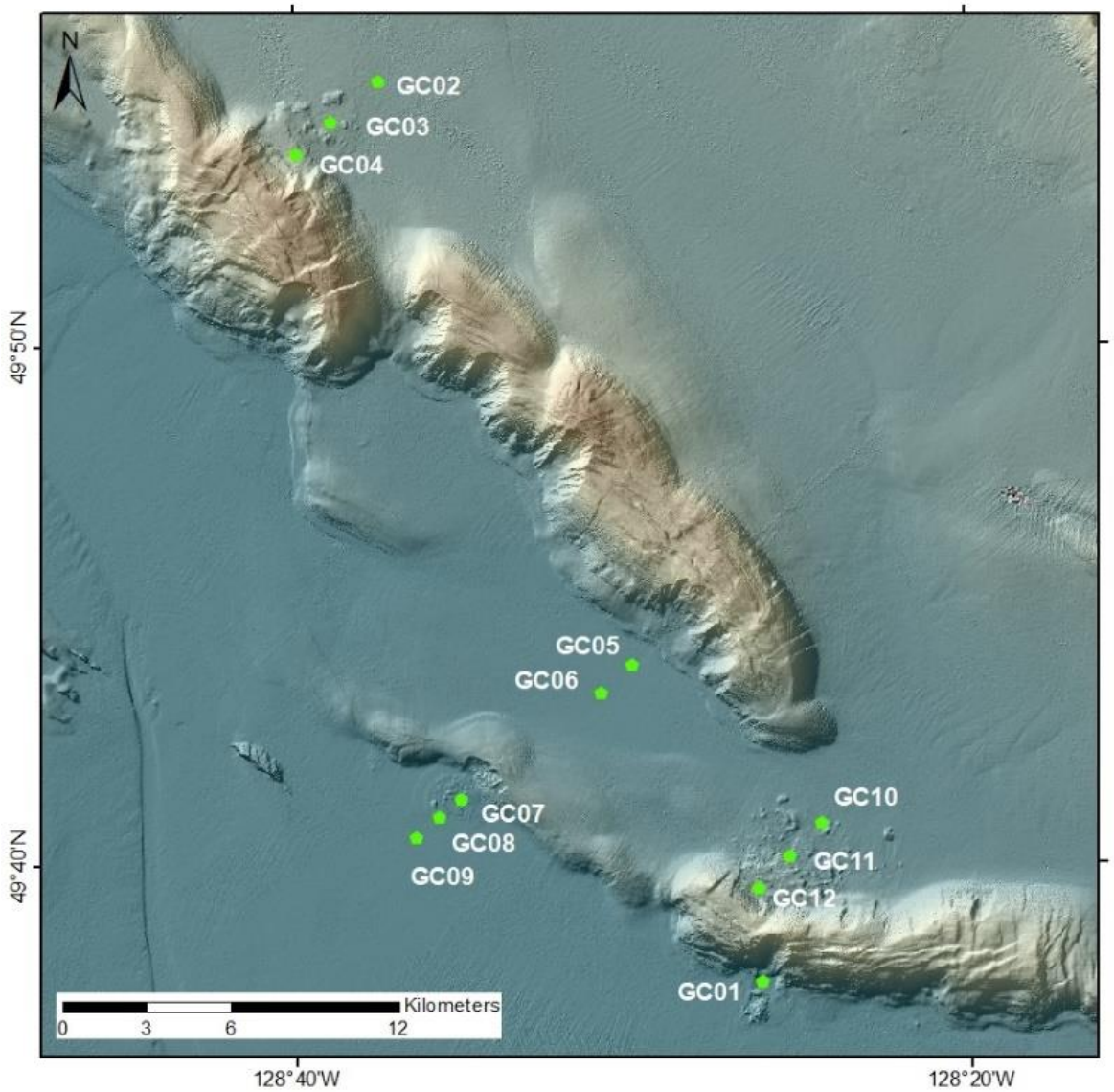

Figure 8: Map showing all gravity cores taken at submarine slope failures in the Winona Basin.

All on board are well and send greetings home.

Michael Riedel (on behalf of all participants of Expedition CLOCKS)

(GEOMAR Helmholtz Center for Ocean Research Kiel)